Electrocatalytic CO_2 Reduction with a Membrane Supported Manganese Catalyst in Aqueous Solution

James J. Walsh,[a] Gaia Neri[a], Charlotte L. Smith[a] and Alexander J. Cowan*[a]

Electronic supplementary information

Contents:

1. Experimental:

1.1 Materials: Bromopentacarbonylmanganese(I) (Sigma-Aldrich), 2,2'-bipyridine (bpy) (Sigma-Aldrich), acetonitrile (chromatographic grade, Sigma-Aldrich), Nafion (5 % w/w in lower alcohols, Sigma-Aldrich), sodium phosphate monobasic (≥ 99 %, Sigma-Aldrich), sodium phosphate dibasic (≥ 99 %, Sigma-Aldrich), multi-walled carbon nanotubes (MWCNT >98% carbon, 6-13 nm × 2.5-20 μm, Sigma-Aldrich) and tetrabutylammonium perchlorate (Sigma-Aldrich) were used as received. Milli-Q water (18.2 MΩ) was used for all aqueous solutions. CO_2 and argon (CP grade) were purchased from BOC. Helium (N6.0) was purchased from BOC. The calibrant gas for the GC was a custom ordered mixture of 500 ppm H_2 and 200 ppm CO in helium and was purchased from STG.

[Mn(bpy)(CO)$_3$Br] was synthesized according to literature methods.[1] The synthesis was conducted completely in the absence of light by covering all reflux apparatus in aluminium

foil prior to addition of reagents and under a N_2 atmosphere. $Mn(CO)_5Br$ (200 mg, 0.72 mmol) and 2,2'-bipyridine (115 mg, 0.74 mmol) were dissolved in 30 ml diethyl ether and refluxed for 3 hours at 40°C. The mixture was left to cool overnight, resulting in the formation of an orange powder precipitate. The product was removed from the mother liquor by cooling in an acetone-dry ice bath for 2 hours. The orange powder was filtered off and rinsed with cold diethyl ether until the solvent ran colourless. The product was left on a vacuum pump for 48 hours to dry. Yield = 61%; ^{1}H-NMR (CD_3CN ,400 MHz): d = 9.22 (d, *J*=5.5 Hz, 2 H), 8.34 (d, *J*=8.0 Hz, 2 H), 8.12 (t, *J*=1.0 Hz, 2 H), 7.61 ppm (t, *J*=6.5 Hz, 2 H); ^{13}C-NMR (CD_3CN, 101 MHz): d = 155.7, 154.1, 139.6, 127.1, 123.6 ppm; FTIR (CH_3CN): 2027, 1934, 1922 cm^{-1}; Anal. calcd. for $C_{13}H_8BrMnN_2O_3$: C, 41.64; H, 2.15; N, 7.46. Found: C, 41.59; H, 2.06; N, 7.34.

1.2 Film preparation: The membrane was prepared from [$Mn(bpy(CO)_3Br$] (typically 5.5 mg) dissolved in 0.5 ml of acetonitrile, mixed with 0.5 ml a Nafion/alcohol solution (5.0 % w/w) in a 1:1 volume ratio in the dark. In a typical experiment 10 µl (corresponding to 140 nmol of [$Mn(bpy(CO)_3Br$] in 2.5 % Nafion/MeCN 1:1) of this yellow solution was transferred onto a polished glassy carbon electrode using an autopipette and left to dry in air in the dark for several hours, yielding a pale yellow polymer film that completely coated the working area. Prolonged CPE experiments (Fig. S5) used only 5 µl of the casting solution, corresponding to 70 nmol of catalyst deposited. Casting solutions for MWCNT/Nafion/[$Mn(bpy)(CO)_3Br$] films were prepared as above with the addition of MWCNT (5.5 mg) to the casting solution, that was then sonicated in the dark for 15 minutes. 5 µl of this darkly coloured casting solution was then transferred onto a polished glassy carbon electrode using an autopipette and left to dry in air in the dark for several hours

1.3 Apparatus: All electrochemistry was performed with a PalmSens^3 potentiostat. Gas chromatography was performed using an Agilent 6890N employing N6 helium as the carrier gas (5 $ml.min^{-1}$). A 5 Å molecular sieve column (ValcoPLOT, 30 m length, 0.53 mm ID) and a pulsed discharge detector (D-3-I-HP, Valco Vici) were employed. CO and H_2 peak areas were quantified with multiple calibrant gas injections and were re-calibrated daily. NMR spectra were recorded on a Bruker Advance 400 NMR spectrometer with CD_3CN as the solvent and an amber quartz NMR tube. ESI MS and elemental analyses were performed by the University of Liverpool analytical services. FTIR spectra were recorded using a JASCO 4000 FTIR. Scanning electron microscopy of films cast on glass slides was recorded using a Jeol 6610 SEM operating at an accelerating voltage of 20 kV. Profilometry was measured using an Ambios Technology XP200.

1.4 Electrocatalysis: The electrolyte was a phosphate buffer (30 mM Na_2HPO_4 + 30 mM NaH_2PO_4 in Milli-Q water). The electrolyte was pH = 7.0 when air saturated and pH = 6.2 when CO_2 saturated. Cyclic voltammograms of the catalyst films were performed in a pear-shaped flask with a glassy carbon disc working electrode (BASi, geometric surface area = 0.0717 cm^2), a Pt basket counter electrode and a Ag/AgCl (3 M NaCl) reference electrode (BASi). All CV and CPE experiments were performed in the dark as the Mn complex is photosensitive. The flask was purged with either argon or CO_2 for 20 minutes prior to scanning. Controlled potential electrolysis (CPE) was performed in a custom made pyrex H-cell with the two compartments separated by a fine glass frit. The same electrodes as above were used but with an extra double junction (porous glass frit) covering the Pt counter electrode to minimize re-oxidation of CO or other reaction products. Both compartments were magnetically stirred throughout the CPE reaction. Results presented are based on an average of at least two independent measurements, with typical variability of ~ ± 10 % in product yields with ~3.5 x 10^{-10} mol of electroactive catalyst. It was noted that in the selectivity and activity was highly dependent upon the coverage of the GCE by the Nafion film and the electroactive concentration, making it important to ensure that the entire GCE surface is covered and that no cracks in the membrane occur upon drying. The faradaic efficiencies (FE) achieved were calculated by taking the measured product yields (GC) and charge passed (Q) and accounting for the requirement of 2 electrons to produce one CO molecule.

$$FE_{CO}\ (\%) = \left[\frac{\mathrm{CO}\ (mol)}{\left[{}^{Q(C)}/_{2\times 96485\ (C\ mol^{-1})}\right]}\right] \times 100$$

$$TON_{CO} = \frac{\mathrm{CO}\ (mol)}{electroactive\ catalyst\ (mol)}$$

The overall FE for all gas phase products measured (H_2 + CO) was 75 % and 69 % in the Nafion/[Mn(bpy)$(CO)_3$Br] at -1.5 V and MWCNT/Nafion/[Mn(bpy)$(CO)_3$Br] at -1.4 V CPE experiments respectively. Given the theoretical maximum total FE is 100% it is possible to calculate the maximum possible concentration of a liquid phase products produced during CPE. For the Nafion/[Mn(bpy)$(CO)_3$Br] at -1.5V:

Q = 63 mC, $FE_{(H2+CO)}$= 75 %

$\therefore$ the unaccounted charge = 0.25 x 63 mC = 15.75 mC

Liquid phase CO_2 reduction products may include:

- $CO_2 + 2H^+ + 2e^- \rightarrow HCO_2H$
- $CO_2 + 4H^+ + 4e^- \rightarrow HCHO + H_2O$
- $CO_2 + 6H^+ + 6e^- \rightarrow CH_3OH + H_2O$

The highest concentration of a liquid phase CO_2 reduction product would be *via* a 2 electron pathway (e.g. HCO_2H formation). 15.75 mC would lead to a maximum product yield of 82 nmol. The total electrolyte volume of the cell is 23 ml, leading to a maximum concentration of ~3 μM for liquid phase CO_2 reduction products.

2. Catalyst and Membrane Characterisation:

2.1 CV of solution phase [Mn(bpy)(CO)$_3$Br]:

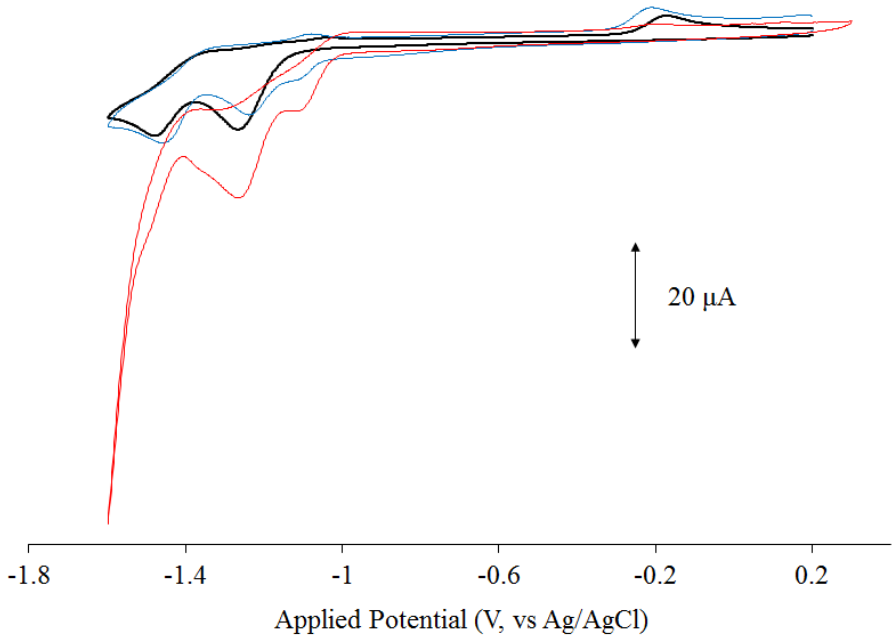

Fig. S1: CVs of [Mn(bpy(CO)$_3$Br] in 0.1 M (But)$_4$NClO$_4$/MeCN at 100 mV.s^{-1}. Black: Ar, blue: Ar + 5 % H_2O, red: CO_2 + 5 % H_2O. Under Argon the first reduction at -1.26 V vs Ag/AgCl is assigned to reduction of the [Mn(bpy(CO)$_3$Br]. The introduction of water leads to a new shoulder peak at less negative potentials ca. -1.07 V vs Ag/AgCl previously assigned to the reduction of [Mn(bpy(CO)$_3$CH$_3$CN]$^+$.[1]

2.2 Spectroscopic and electrochemical analysis of Nafion/[Mn(bpy)(CO)$_3$Br]:

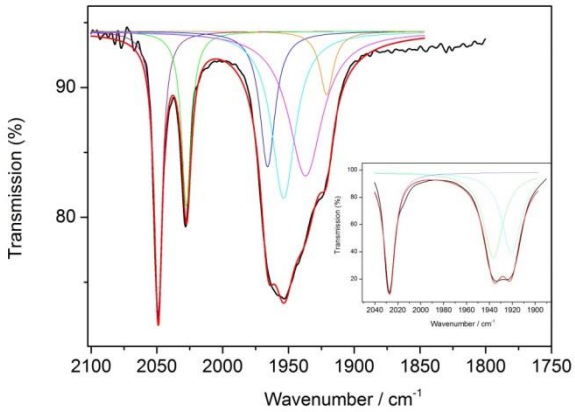

Fig. S2: FTIR spectra of [Mn(bpy)(CO)$_3$Br] in CH$_3$CN/Nafion solution (black) approximately 30 minutes after mixing. Multi-Lorentzian fitting curve is shown with the overall fit in red alongside the individual Lorentzian peaks. Inset shows [Mn(bpy)(CO)$_3$Br] in CH$_3$CN for reference.

FTIR analysis and multi-Lorentzian fitting shows the presence of the [Mn(bpy)(CO)$_3$Br] ν(CO) stretches at 1921, 1937 and 2027 cm^{-1}, which were recorded independently (figure inset) and have been previously reported elsewhere,[1,2] as well as three new ν(CO) stretches at 2049, 1965 and 1953 cm^{-1} which are assigned to the formation of [Mn(bpy)(CO)$_3$(solv)]$^+$ (where solv = CH$_3$CN, H$_2$O or *n*-propanol), in agreement with previous reports.[1,3] Assuming similar extinction coefficients for the ν(CO) of [Mn(bpy)(CO)$_3$(solv)]$^+$ and [Mn(bpy)(CO)$_3$Br], it is possible to use the fitting parameters from figure S2 to estimate the relative concentration of [Mn(bpy)(CO)$_3$(solv)]$^+$ (ca. 55%) in the Nafion system. It is noted that the assumption of similar extinction coefficients may introduce significant error into this calculation, and the UV/Vis experiments (Fig S3) indicate that 55% may be a lower limit as in Nafion we observe an excellent agreement with the reported UV/Vis spectrum of pure [Mn(bpy)(CO)$_3$(CH$_3$CN)]$^+$.[1]

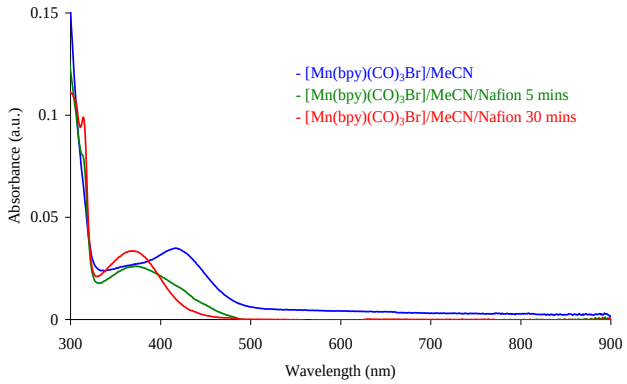

Fig. S3: UV/Vis spectra of [Mn(bpy)(CO)$_3$Br] in MeCN (blue) or MeCN/Nafion solution (green, red). Spectra show that ligand exchange in the dark appears to be promoted in the presence of Nafion.

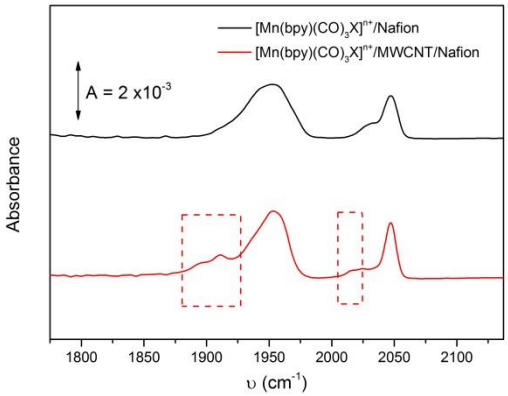

Fig. S4: FTIR spectra of [Mn(bpy)(CO)$_3$X]$^{n+}$ dried Nafion film (black) and in a MWCNT/Nafion film. The inset shows the Multi-Lorentzian fitting curves for the Nafion/MWCNT/[Mn(bpy)(CO)$_3$Br] sample. ν(CO) for a new carbonyl complex formed in the presence of MWCNT are highlighted.

The sensitivity of the frequency of ν(CO) measured by FTIR provides an excellent probe of the electron density at the metal centre. In addition to the ν(CO) bands of [Mn(bpy)(CO)$_3$Br] and [Mn(bpy)(CO)$_3$(MeCN)]$^+$ reported in Figure S2 we also observed the formation of a low concentration of a new Mn carbonyl species with ν(CO) at *ca*. 2016, 1910 and 1896 cm^{-1} upon incorporation of MWCNT into a [Mn(bpy)(CO)$_3$Br]/CH$_3$CN/Nafion solution. We are able to rule out the presence of the known dimer [Mn(bpy)(CO)$_3$]$_2$ which has ν(CO) at 1975 (m), 1963 (w), 1936 (s), 1886 (m) and 1866 (m) cm^{-1} in THF[4] and the relative splitting of the new ν(CO) peaks indicates the presence of a new tricarbonyl formed upon interaction with the MWCNT. The presence of the new species may be indicative of a non-covalent interaction between the MWCNT and the [Mn(bpy)(CO)$_3$X]$^{n+}$; however further studies, which

are beyond the scope of this initial communication, would be required to identify the nature of these interactions. Interestingly we do note that the ν(CO) stretches of the new tricarbonyl occur at lower wavenumbers than those of both $[Mn(bpy)(CO)_3(CH_3CN)]^+$ and $[Mn(bpy)(CO)_3Br]$, but higher than those of the doubly reduced species $[Mn(bpy)(CO)_3]^-$ (1916, 1815 (br) cm^{-1}),[4] suggesting an electron density at the Mn centre in the presence of MWCNT that is significantly higher than in the absence of MWCNT, but still well below that present in the doubly reduced complex.

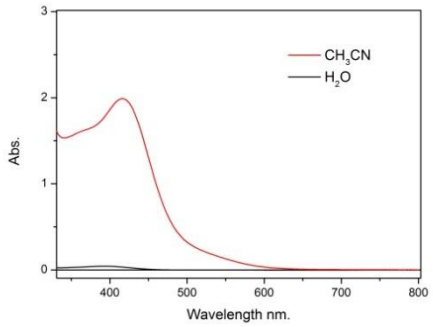

Fig. S5: UV/Vis of $[Mn(bpy)(CO)_3Br]$ 1 mM in CH_3CN. Same mass of $[Mn(bpy)(CO)_3Br]$ suspended in water, stirred for 1 hour then centrifuged, showing the lack of solubility of the complex in water.

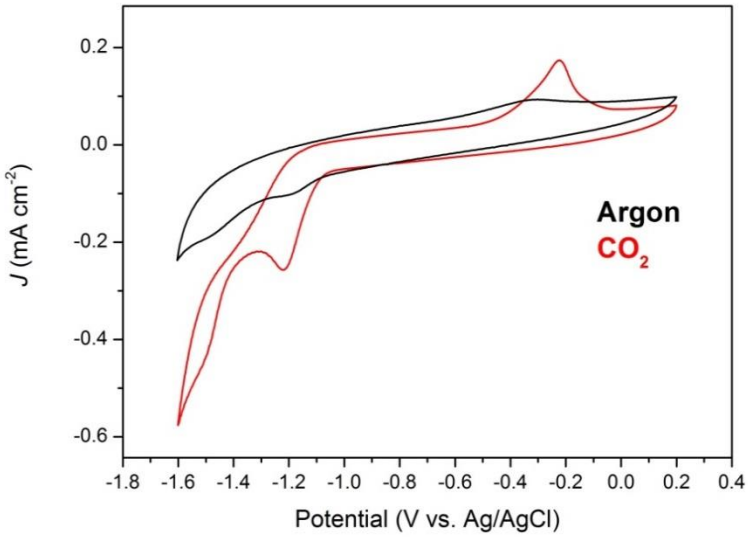

Fig. S6: Cyclic voltammograms of $[Mn(bpy(CO)_3Br]$ cast in a Nafion film on glassy carbon (d = 3 mm). The reference electrode was Ag/AgCl and the counter a Pt basket. Electrolyte was aqueous 30 mM Na_2HPO_4 + 30 mM NaH_2PO_4 buffer at pH ~ 7.0 Argon (black) or CO_2 (red). 100th scans shown. v = 100 mV.s^{-1}

2.3 Scan rate dependence

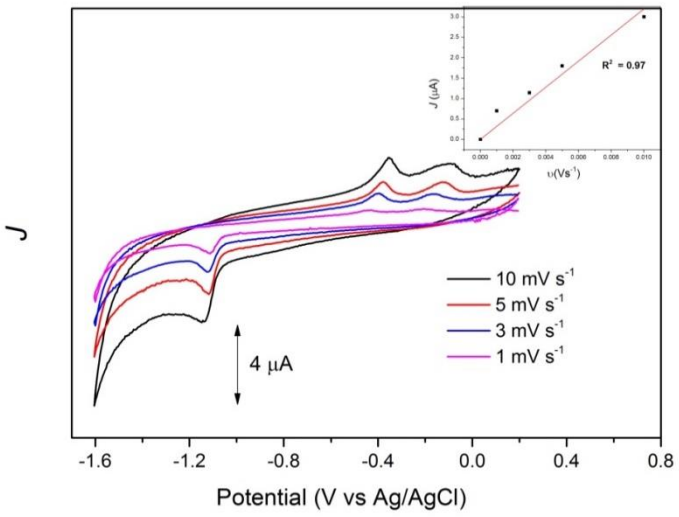

Fig. S7: Slow scan rate CVs of 10 µl film on glassy carbon disc (140 nmol [Mn(bpy)(CO)$_3$Br] deposited onto a GCE (0.07 cm^2) in argon purged 60 mM phosphate buffer. Inset: Plot of scan rate vs peak current for the first Mn reduction.

A linear dependence of peak current for the reduction of $[Mn(bpy)(CO)_3X]^{n+}$ at -1.15 V to the scan rate is measured indicating that a surface immobilised redox process is occurring, in line with expectations for a membrane supported electro-active species. Using the relationship[5]:

$$i = \frac{(n^2F^2\nu A\Gamma)}{4RT}$$

Where n is the number of electrons transferred, F is Faraday's constant, ν is the scan rate in V s^{-1}, A the electrode surface area (cm^2), Γ the surface coverage (mol cm^{-2}), R the gas constant (J mol^{-1}K^{-1}) and T the temperature (K), it was possible to calculate a typical surface electro-active coverage of catalyst of ~3.5 x10^{-10} mol in the experiments where 140 nmol of catalyst were dissolved in the casting solution. The concentration of electroactive material in the MWCNT sample was assessed through analysis of the dimer re-oxidation, at *ca.* -0.5 V as the 2 successive reductions under argon are found to be heavily overlapped, using the relationship between surface coverage and charge:

$$\Gamma = \frac{Q}{nFA}$$

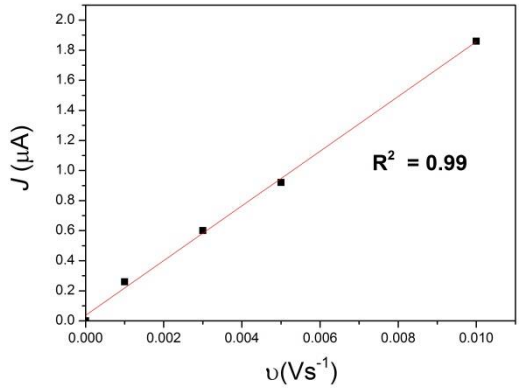

Fig. S8: Plot of scan rate vs peak current for the re-oxidation of $[Mn^{0}(bpy)(CO)_3]_2$ *at ca. -0.4 V.*

2.4 Film morphology

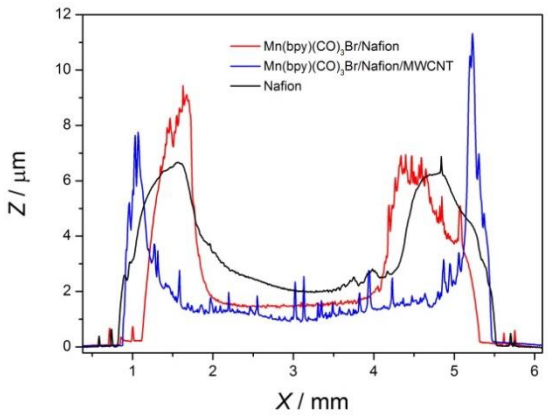

Fig. S9: Profilometry of Nafion, Nafion/[Mn(bpy)(CO)$_3$Br] and Nafion/[Mn(bpy)(CO)$_3$Br]/MWCNT membranes. It is interesting to note the presence of small micron sized clusters on both the Nafion/[Mn(bpy)(CO)$_3$Br] and MWCNT/ Nafion/[Mn(bpy)(CO)$_3$Br] membranes.

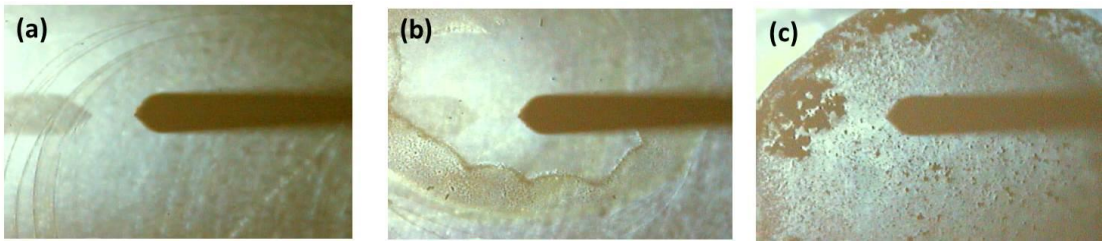

Fig. S10: Optical images of (a) Nafion film, (b) [Mn(bpy)(CO)$_3$Br]/Nafion and (c) [Mn(bpy)(CO)$_3$Br]/MWCNT/Nafion recorded during profilometry.

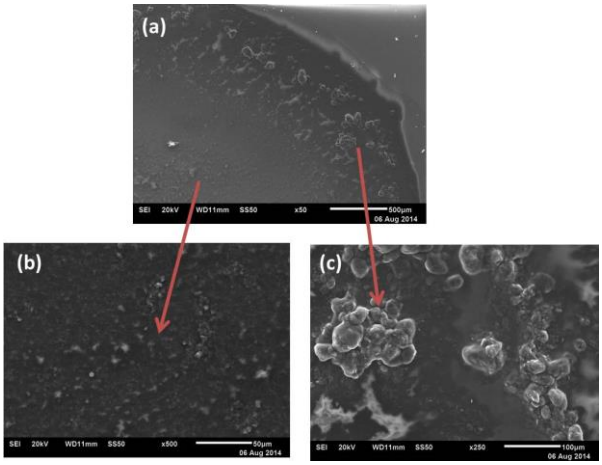

Fig. S11: SEM of Nafion/[Mn(bpy)(CO)$_3$Br]/MWCNT films, showing a magnification of the clusters found at the film edges and the centre of the film.

The measured electroactive concentration, the confirmation of surface confined electrochemistry and the film morphology studies are of relevance when considering the mechanism of dimer formation within a Nafion film. Several mechanisms can be proposed (1) diffusion of the Mn species through the Nafion channels, (2) diffusion of the Mn complex into solution following leaching and (3) the presence of closely packed Mn complexes in localized clusters that do not require diffusion for dimerization. We favour the 3rd hypothesis for the following reasons:

(i) Both (1) and (2) require the movement of electroactive $Mn(bpy)(CO)_3X]^n$. The linear scan rate dependence of the peak current for both the reduction of $[Mn(bpy)(CO)_3X]^n$ (Fig. S8) and the re-oxidation of the dimer (Fig. S9) indicate that a surface immobilised redox process is occurring this allows us to rule out rapid free diffusion (on the CV timescales studied) of $[Mn(bpy)(CO)_3X]$ through either the Nafion channels (∅~2.4 nm)[6] or solution.

(ii) Figures S14-S17 clearly show that no $[Mn(bpy)(CO)_3X]^n$ species are found in the post electrolysis electrolyte, in-line with expectations for a catalyst insoluble in aqueous solutions, ruling out the mechanism (2) and the possibility of the Mn complexes being dissolved, transported or leached back out of the membrane.

(iii) The formation of clusters of $[Mn(bpy)(CO)_3X]^n$, required for the 3rd mechanism, is probable given that the when the volatile organic solvents (CH_3CN, propanol) are removed through drying during film preparation, the $[Mn(bpy)(CO)_3Br]$ will precipitate out leading to small deposits within the Nafion membrane. Catalyst aggregates have also been previously reported for a related $[Re(bpy)(CO)_3Br]$ system.[7] Optical images (Fig. S10(b)) shows that yellow clusters appear to be localised at the film edges, and profilometric data (Fig. S9) shows enhanced roughness upon the inclusion of $[Mn(bpy)(CO)_3Br]$. SEM images (Fig. S11) of the MWCNT/$[Mn(bpy)(CO)_3Br]$ membrane also show the presence of large clusters at the film edge which may be either MWCNT bundles or the $[Mn(bpy)(CO)_3X]^{n+}$.

(iv) In the absence of fast catalyst diffusion (mechanism (3)) we would anticipate that only Mn clusters close to the GCE interface within the Nafion in the absence of MWCNT would be electrochemically active, in line with our reported very low measured concentrations of electrochemically active catalyst (Figs. S7, S8). This is due to Nafion being a poor conductor of electrons. A mobile catalyst within the Nafion would be expected to lead to higher concentrations of electrochemically active species. The inclusion of MWCNT effectively increases the electrode surface area making it more probable that a Mn cluster is close to the electro-active surface leading to higher electroactive concentrations and current densities.

2.5 MWCNT loading

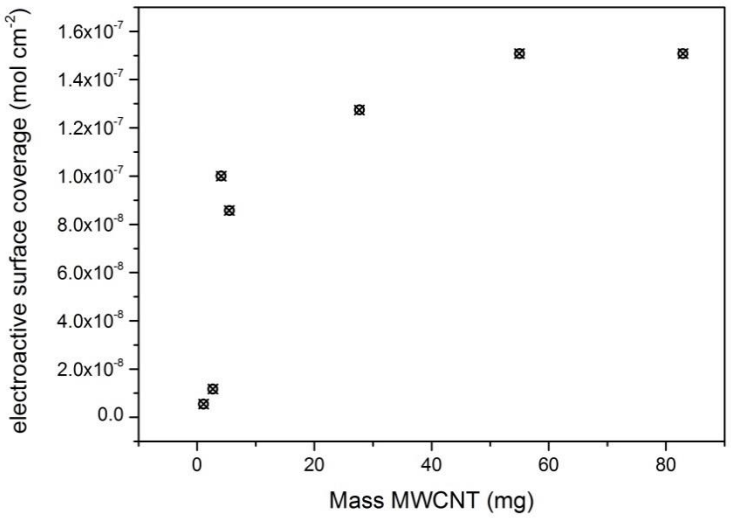

Fig. S12: Effect of loading on the measured electroactive concentration of [Mn(bpy)(CO)$_3$Br] for membranes. Prepared by casting a 5 μl solution containing the indicated mass of MWCNT, 5.5 mg of [Mn(bpy)(CO)$_3$Br] (70 nmol) in 1 ml of a 1:1 acetonitrile/Nafion/ solution (2.5 % w/w).

3. Electrocatalysis

3.1 Control experiments

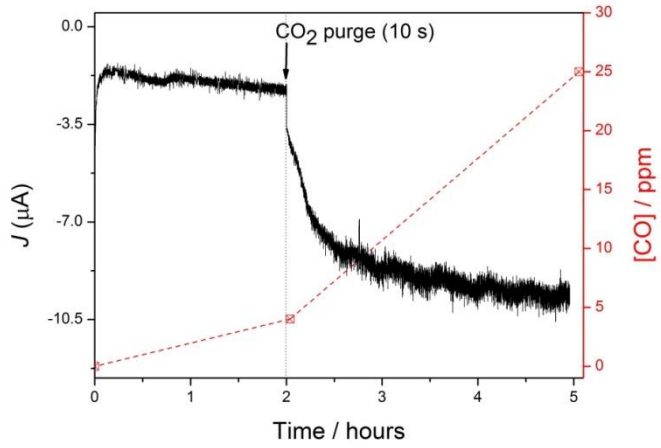

Fig. S13: Amperometric detection (black) of a [Mn(bpy)(CO)$_3$Br] (140 nmol)/Nafion film in 30 mM Na_2HPO_4 + 30 mM NaH_2PO_4 buffer at pH ~ 7.0 held at -1.5 V vs Ag/AgCl. The experiment is initially carried out under an Argon atmosphere before CO_2 is briefly introduced (10 s purge). GC headspace analysis (red) of the electrochemical cell at the reaction start, immediately prior to CO_2 introduction and at the reaction end clearly showing a large increase in the rate of CO production upon introduction of the CO_2.

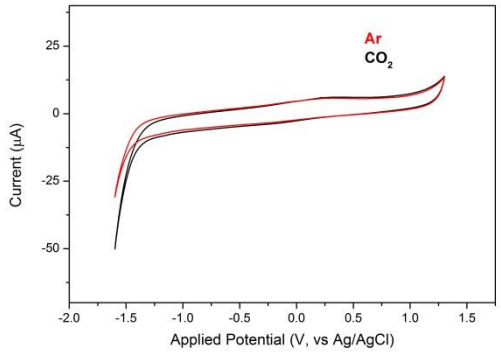

Fig. S14: CV of post CPE electrolyte (from [Mn(bpy)(CO)$_3$Br]/Nafion membrane held at -1.5 V for four hours) with a clean glassy carbon electrode under Argon and CO_2, confirming that no electroactive materials are leached out of the membrane during experiments.

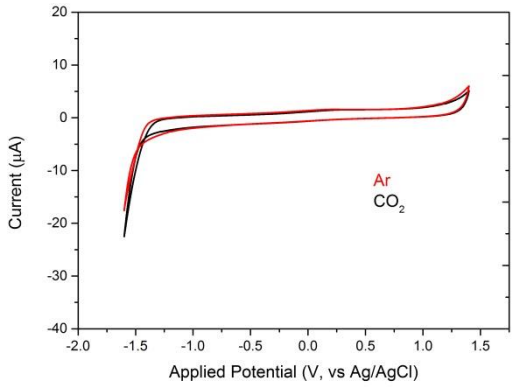

Fig. S15: CV of post CPE electrolyte (from [Mn(bpy)(CO)$_3$Br]/MWCNT/Nafion membrane held at -1.25 V for four hours) with a clean glassy carbon electrode under Argon and CO_2, confirming that no electroactive materials are leached out of the membrane during experiments.

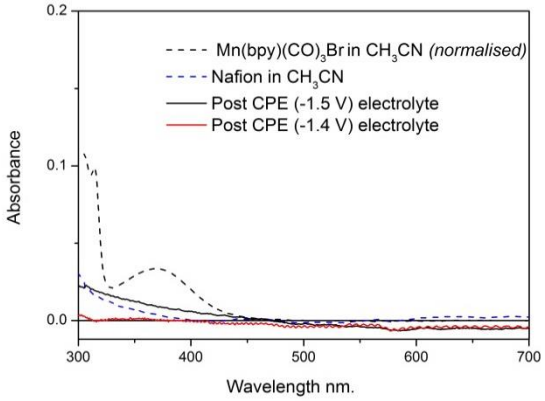

Fig. S16: UV/Vis spectra of [Mn(bpy)(CO)$_3$Br] in solution, Nafion solution (dashed lines) and the electrolyte solutions post CPE of [Mn(bpy)(CO)$_3$Br]/Nafion membranes at the

potential indicated. UV/Vis indicates that no [Mn(bpy)(CO)$_3$Br] is leached out of the membrane during CPE experiments.

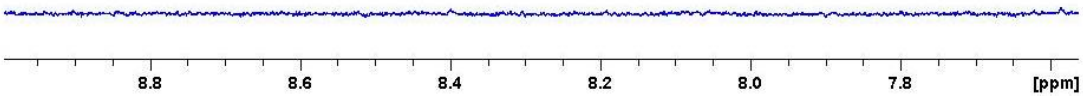

Fig. S17: ^{1}H-NMR spectrum of electrolyte content following CPE (-1.5 V) of a Nafion/[Mn(bpy)(CO)$_3$Br] membrane (CPE described in main text Fig. 2), which was evaporated to a solid and re-dissolved in minimal CD$_3$CN. The post-electrolysis solutions show the presence of no [Mn(bpy)(CO)$_3$Br] (see ESI 1.1 for known shifts).

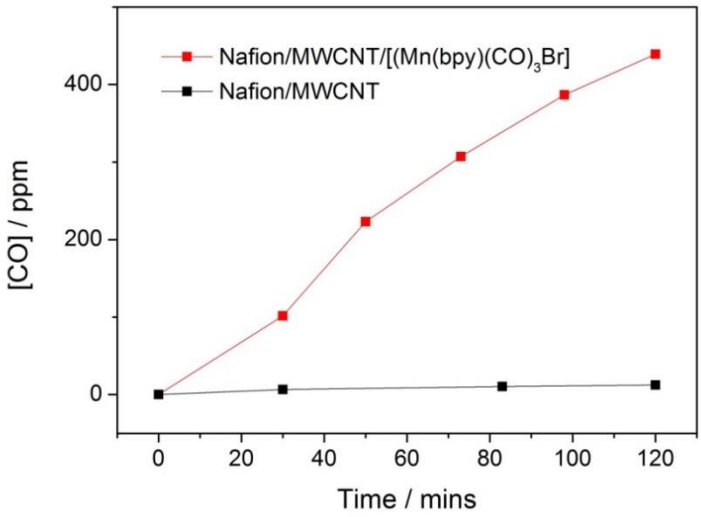

Fig. S18: Gas headspace analysis for CPE of a Nafion/MWCNT/[Mn(bpy)(CO)$_3$Br] and Nafion/MWCNT film both on a GCE at -1.4 V, 60 mM phosphate buffer, CO$_2$ purged, showing that the [Mn(bpy)(CO)$_3$Br] complex is required for electrocatalytic CO$_2$ reduction

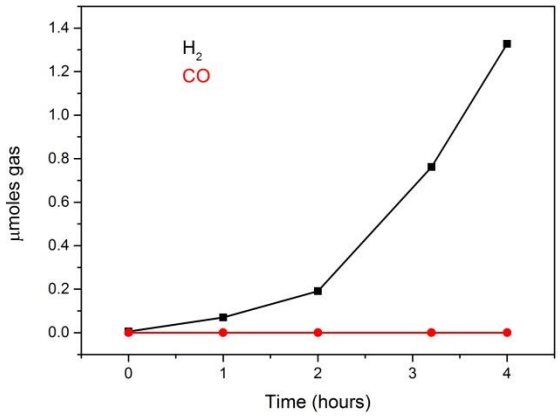

Fig S19: Gas headspace analysis for CPE of a Nafion/MWCNT/[Mn(bpy)(CO)$_3$Br] on a GCE at -1.4 V, 60 mM phosphate buffer, argon purged, showing that CO_2 is require for CO production.

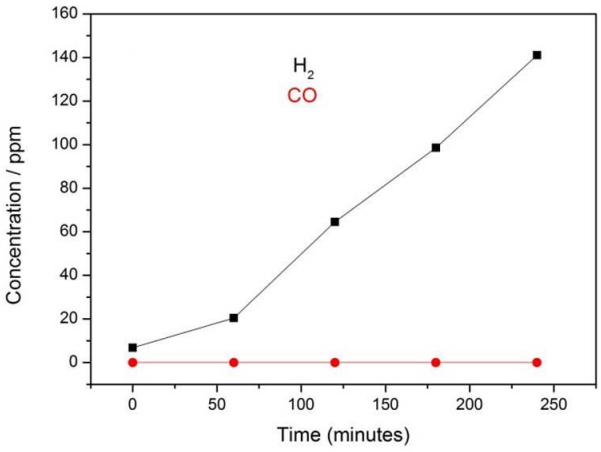

Fig. S20: Gas headspace analysis for CPE analysis of a Nafion film on a GCE at -1.5 V, 60 mM phosphate buffer, CO_2 purged, showing that the [Mn(bpy)(CO)$_3$Br] complex is required for electrocatalytic CO_2 reduction.

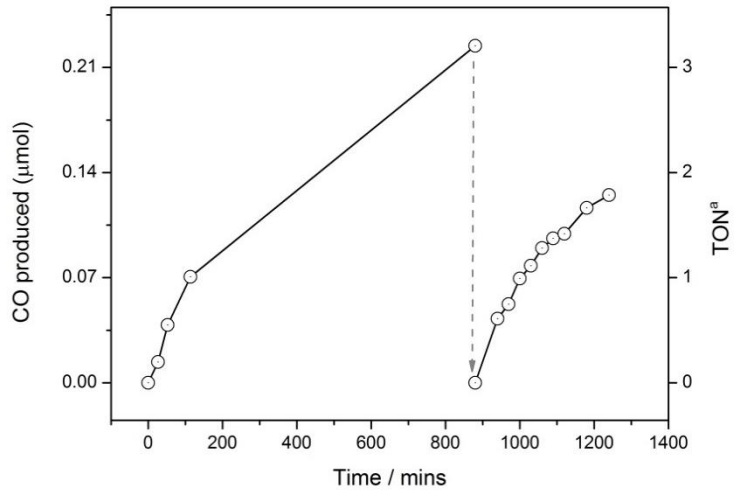

Fig. S21. The overall TON for CO is ca. 5 (70 nmol of [Mn(bpy)(CO)$_3$Br] deposited onto a GCE (0.07 cm^2) in a 5 µl solution (1:1 Nafion (2.5%wt):CH$_3$CN)), during CPE at -1.5 V vs. Ag/AgCl in a CO$_2$ purged 60 mM phosphate buffer (pH~7). The TON is well in excess of that achievable by catalyst decomposition. The sample was run for a period of 880 minutes, then briefly repurged with CO$_2$ (grey dashed line) prior to the experiment resuming. [a]TON are based on the total amount of [Mn(bpy)(CO)$_3$Br] deposited and not the electroactive content of the film.

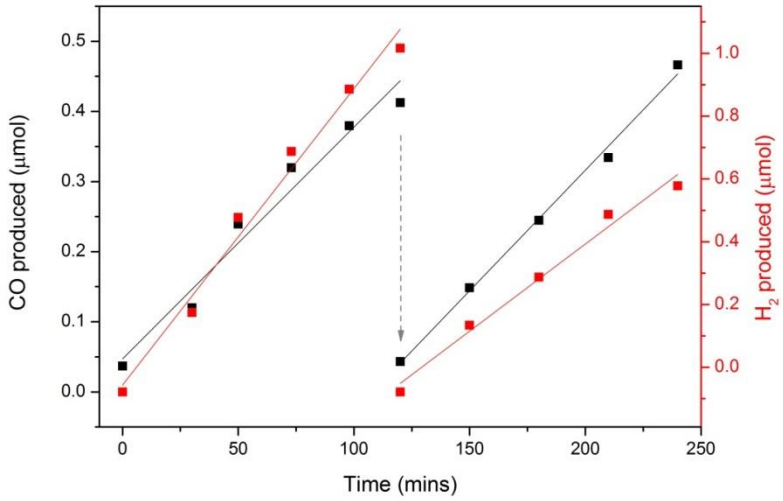

Fig. S22: The overall TON for CO is 14 (70 nmol of [Mn(bpy)(CO)$_3$Br] deposited onto a GCE (0.07 cm^2) in a 5 µl solution (1:1 Nafion (2.5%wt):CH$_3$CN) with MWCNT present (1:1 wt to [Mn(bpy)(CO)$_3$Br]), held at -1.4 V vs. Ag/AgCl in a CO$_2$ purged 60 mM phosphate buffer (pH~7). The TON is well in excess of that achievable by catalyst decomposition. The sample was run for a period of 120 mins before being briefly repurged with CO$_2$ (grey dashed line). H$_2$:CO selectivity was maintained close to 2:1 throughout the experiment.

3.2 Catalyst benchmarking:

The activity of the Nafion/[Mn(bpy)$(CO)_3$Br] catalysts reported can be directly compared to those previously reported for the related Nafion/[Re(bpy)$(CO)_3$Br] system once normalised for surface area of GCE, Table 1 main text.[7] Compared to the rhenium analogue we find higher TON and improved selectivities are achieved with Mn at -1.4 to -1.5 V vs Ag/AgCl in addition to the presence of catalytic activity at lower applied potentials. Direct benchmarking between the activity of the homogenous [Mn(bpy)$(CO)_3$Br] system[1] and the heterogeneous Nafion immobilised catalyst by comparison of overall TON in a defined time period is however not appropriate. It has recently been highlighted by Savéant and co-workers[8,9] that a fair activity comparison between heterogeneous and homogenous systems requires the consideration of only the catalyst concentration present in a reaction layer close to the electrode surface in the homogenous experiment. If this is not done the TOF reported for the homogenous systems will be greatly disadvantaged due to the presence of the bulk catalyst and furthermore TOF obtained will be highly dependent upon the volume-surface ratio of the cell used. For example it was reported that bulk electrolysis over 22 hours of [Mn(bpy)$(CO)_3$Br] (2.5 x10^{-5} mol of catalyst) at *ca*.-1.35 V vs Ag/AgCl led to Q = 130 C being passed with a FE of 85% for CO,[1] which we calculate to be a TON ~ 23, giving a bulk TOF ~ 0.0003 s^{-1} which is well below the real TOF = 0.45 s^{-1} (log TOF = -0.35 s^{-1} at η = 0.51 V) calculated by Savéant *et al*. using a foot-of–the-wave analysis of CV data.[9]

Figure S10 shows the TOF for our heterogeneous system calculated from the CPE data reported in the main text. As can be seen from figure S10, we report significantly lower TOF for the Nafion immobilised system compared to the homogenous solution at a similar overpotential (η ~ 0.6 V). As noted in the main text the diffusion of CO_2 is likely to be a major limiting factor in these polymer immobilised materials. It is also highly desirable to be able to compare the extrapolated TOF at η = 0 V between two systems; however the TOF_0 in Nafion (log TOF_0 ~ -3.0 s^{-1} *cf.* -8.7 s^{-1} for [Mn(bpy)$(CO)_3$Br] in CH_3CN + 5% H_2O) is believed to be artificially high as unlike the foot-of the-wave method we are unable to account for how the concentration of CO_2 within Nafion varies with potential and time during our CPE measurement.

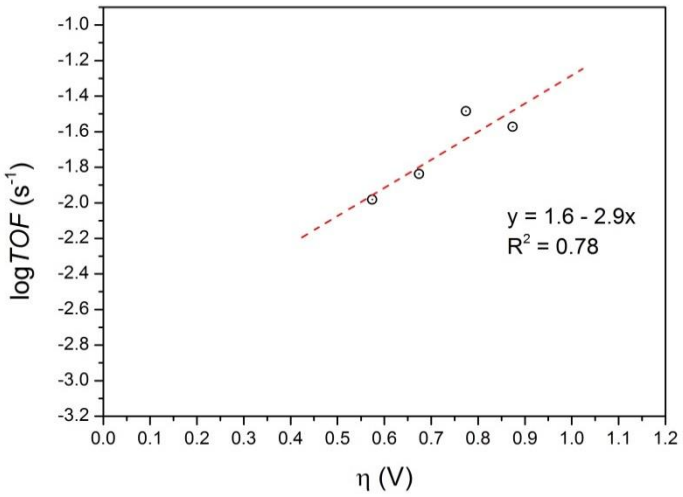

Fig. S23: Measured dependence of TOF (from preparative scale electrolysis) with overpotential for Nafion/[Mn(bpy)(CO)$_3$Br] in pH 7 electrolyte. The experimental data presented is likely to be strongly affected by variations in C_{CO2} within the Nafion membrane.

References:

1. M. Bourrez, F. Molton, S. Chardon-Noblat and A. Deronzier, *Angew. Chem. Int. Ed. Engl.*, 2011, **50**, 9903–9906.
2. J. M. Smieja, M. D. Sampson, K. A. Grice, E. E. Benson, J. D. Froehlich and C. P. Kubiak, *Inorg. Chem.*, 2013, **52**, 2484–91.
3. J.-D. Compain, M. Bourrez, M. Haukka, A. Deronzier and S. Chardon-Noblat, *Chem. Commun.*, 2014, **50**, 2539–42.
4. F. Hartl, T. Mahabiersing, P. Le Floch, F. Mathey, L. Ricard, P. Rosa and S. Záliš, *Inorg. Chem.*, 2003, **42**, 4442–4455.
5. Bard, A. J. and Faulkner, L.R., *Electrochemical Methods: Fundamentals and Applications, 2nd Edition*, Wiley, 2nd edn., 2001.
6. K. Schmidt-Rohr and Q. Chen, *Nat. Mater.*, 2008, **7**, 75–83.
7. T. Yoshida, K. Tsutsumida, S. Teratani, K. Yasufuku and M. Kaneko, *J. Chem. Soc. Chem. Commun.*, 1993, 631–633.
8. C. Costentin, S. Drouet, M. Robert and J.-M. Savéant, *J. Am. Chem. Soc.*, 2012, **134**, 11235–11242.
9. C. Costentin, M. Robert and J.-M. Savéant, *Chem. Soc. Rev.*, 2013, **42**, 2423–2436.